ChemComm

Cite this: *Chem. Commun.*, 2011, **47**, 5771–5773

www.rsc.org/chemcomm

COMMUNICATION

Graphene oxide hydrogel at solid/liquid interface†

Jiao-Jing Shao, Si-Da Wu, Shao-Bo Zhang, Wei Lv, Fang-Yuan Su and Quan-Hong Yang*

Received 27th February 2011, Accepted 7th April 2011
DOI: 10.1039/c1cc11166c

A strong solid/liquid interfacial interaction is found between porous alumina and graphene oxide (GO) aqueous dispersion, which promotes a fast enrichment of GO on the alumina surface and results in the formation of a GO hydrogel.

Graphene, as a type of novel but also thinnest material, shows extraordinary electrical,[1] thermal[1c] and mechanical[2] properties and may find applications in many areas, such as biosensors,[3] electrochemical energy storage,[4] solar cells[5] and field emission devices.[6] Graphene oxide (GO) acts as an important precursor for graphene and graphene-based structures,[7] has also received considerable attentions especially from chemists due to its hydrophilic nature of both sides of the graphene basal plane,[8] which makes it processable in aqueous system[7a] and results in many interesting interfacial phenomena.[9] These interfacial phenomena and the resulting GO enrichment at interfaces allow various manipulations of the graphene-based structure in aqueous environment and help realize bottom-up assembly of graphene-based nanoarchitectures and macroforms. Huang *et al.* gave a detailed investigation on various interfacial phenomena of GO,[9c] where GO lowers the surface and interfacial tension due to its amphiphilic nature. We recently reported a liquid/air interfacial enrichment phenomenon of GO,[9a] where a layer-by-layer stacking of GO nanosheets is promoted by evaporation of water upon heating around 80 °C and a thin free-standing membrane is formed. Thus far, most of the investigations focus on the phenomena and assembly processes at liquid/air and liquid/liquid interfaces. In the work mentioned above, Huang *et al.* reported a solid/liquid interfacial interaction between aqueous-dispersed GO and graphite particles or carbon nanotubes, that results in a good dispersion of graphite or nanotubes in the aqueous environment.[9d] To the best of our knowledge, no results have yet been reported on solid/liquid interfacial assembly and the resulting macrostructure of GO.

Here, we report an interesting GO-derived solid/liquid interfacial phenomenon where aqueous-dispersed GO (see ESI† for preparation details) strongly interacts with a hydrophilic porous media, namely anodic aluminium oxide (AAO), to form a hydrogel-like GO-based macrostructure. The interfacial phenomenon derived self-assembly process is quite simple and can be depicted as a GO enrichment onto the porous hydrophilic surface when AAO is immersed into a GO aqueous dispersion, as illustrated in Fig. 1a, by which a concentrated GO hydrogel is finally formed at the solid/liquid interface. The chemically active porous alumina plays a vital role in the interfacial GO enrichment and hydrogel formation.

A GO hydrogel (immersion for 4 h) on the AAO surface and a just removed hydrogel (after immersion for 12 h) are shown as digital photos in Fig. 1b and c, respectively. Fig. 1b demonstrates that a large amount of GO hydrogel is formed on the surface of AAO. From Fig. 1c, it is clearly identified that a hydrogel is mostly formed on the porous side of AAO since this side possesses higher activity than the nonporous one due to the larger surface area. The dynamic rheological behaviour analysis (Fig. S1, ESI†) of an obtained hydrogel reveals that the storage modulus is independent of frequency and higher than the loss modulus across the entire frequency range, indicating that a rheological hydrogel is formed and has

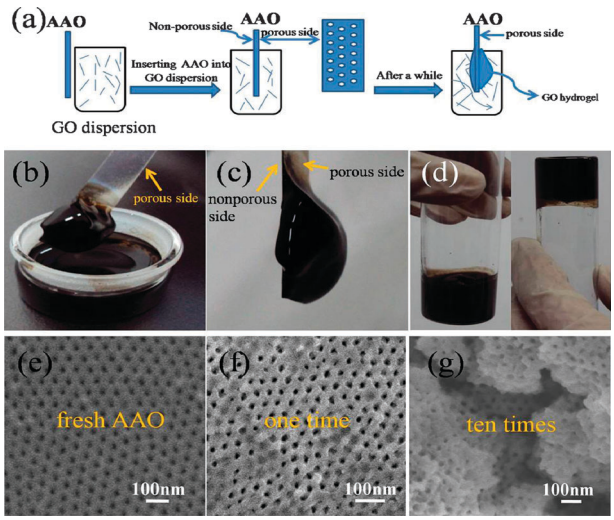

Fig. 1 Formation process of a GO hydrogel. (a) Schematic of the formation process of a GO hydrogel. Digital photos of a hydrogel on the AAO surface (b) and a just removed hydrogel (c). (d) An upturned container test for a GO hydrogel. SEM images of a fresh porous AAO surface (e), AAO surfaces subjected to a single (f) and ten times (g) GO hydrogel formation process. Note that before the SEM observations, the AAO surface was completely washed to remove the formed GO hydrogel.

Key Laboratory for Green Chemical Technology of Ministry of Education, School of Chemical Engineering and Technology, Tianjin University, Tianjin, China. E-mail: qhyangcn@tju.edu.cn; Fax: +86-22-2740-1097; Tel: +86-22-2740-1097

† Electronic supplementary information (ESI) available: Experimental details and supplementary figures. See DOI: 10.1039/c1cc11166c

impressive mechanical properties.[10] A hydrogel that was prepared with an immersion period of 7 days is proved to contain around 99 wt% water (~1 wt% GO) by TGA (Fig. S2, ESI†) and can stand in an upturned container test (Fig. 1d), suggesting that a strong interaction exists among GO sheets even in such a water-abundant hydrogel. It should be noted that the GO fraction of the hydrogel (~1.0 wt%) is apparently higher than that of the as-prepared GO dispersion (~0.2 wt%, see ESI†).

A trace amount of aluminium (~1.8 atom%, C/Al ≈ 38) is unexpectedly found in the hydrogel based on XPS measurements (Fig. S3, ESI†). Fig. 1e–g compares SEM images of an AAO before and after hydrogel formation (the formed hydrogel removed), and it is clearly seen that the hydrogel formation destroys the surface morphology of the alumina. Fig. 1f and g present SEM images of the AAO with different immersion times by employing the AAO for one or ten immersions (around 12 h for each immersion), respectively. The comparative results show that a more severe damage occurs for a longer immersion period. The above results indicate that a strong interfacial interaction occurs between GO and alumina along with the formation of the GO hydrogel.

The influence of temperature on the GO hydrogel formation was also investigated and it was found that a higher temperature is favourable for hydrogel formation. Fig. 2 demonstrates that the thickness of the GO hydrogel formed on the surface of AAO increases gradually with temperature of GO dispersion, implying that the formation of a GO hydrogel is an endothermic chemical process. Moreover, it is noted that a GO hydrogel is only formed in the as-prepared GO dispersion not subject to any further modification to tune the pH value (Fig. S4, ESI†). Since the as-prepared GO dispersion gives an acidic environment (pH = 2.8, for details see ESI†) where alumina is partially transformed to Al^{3+} ions, it is naturally considered that these ions may act as the crosslinkers between GO sheets in the formed hydrogel. However, when we increase the acidity of the dispersion which results in more Al^{3+} ions, unexpectedly, no GO hydrogel was observed at the AAO surface (Fig. S4, ESI†). Therefore, at this stage, it is hard to give an accurate evaluation on the role of Al^{3+} ions in the GO hydrogel formation.

The hydrogel formation is dependent on the surface nature of AAO and GO. On one hand, hydrogel formation is strongly related to the surface area and oxidation degree of alumina. As discussed above, the porous side of AAO (larger surface area) is more active than the nonporous one for hydrogel formation. Meanwhile, only a small amount of GO hydrogel is formed at the surface of slightly oxidized aluminium film (for details see ESI†). On the other hand, the oxygen-containing groups of GO are also crucial for hydrogel formation and the replacement of GO with reduced graphene oxide (RGO) in the presence of surfactant results in no hydrogel formation on the AAO surface. Hydroxyl groups always exist on the surface of metal oxides such as porous AAO (Fig. 3a)[11] while carboxyl groups are one of the main forms of oxygen-containing groups in GO. It is well-known that a strong interaction between hydroxyl and carboxyl groups may result in the formation of a GO hydrogel[12] and a tentative mechanism is proposed as illustrated Fig. 3. GO may be partially ionized to form GO anions and hydrogen cations (Fig. 3b),[13] and the latter would protonate the AAO surface to yield positively charged Brønsted acid sites (Fig. 3c). The GO anions thereafter attack the protonated AAO surface and enrich there to form the GO hydrogel (Fig. 3d), in which GO layers are interlinked with each other by the AAO surface as linkage agents. It is likely that there exists a strong interaction between GO and the AAO surface (partially ionized in acidic environment) as discussed above. When the hydrogel is peeled off from the AAO surface, the alumina surface is clearly damaged as demonstrated above (Fig. 1f and g), and a trace of the partially ionized aluminium component moves into the hydrogel along with the hydroxyl groups on the AAO surface interacting with GO. The detailed mechanism is still unclear at present, especially the role of Al in the hydrogel formation, and further investigations are underway.

The AAO-based GO enrichment suggests a quite simple approach for a macroform with a 3D network by removing the abundant water in the hydrogel. Upon lyophilization for the obtained GO hydrogel the skeleton was well retained in the

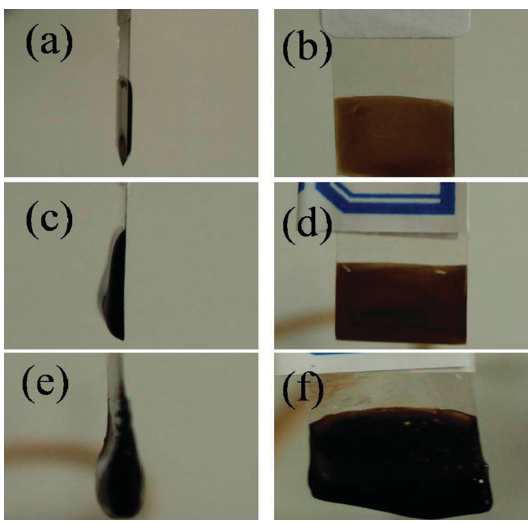

Fig. 2 Influence of temperature on the GO hydrogel formation. Side and front photos of a GO hydrogel at 0 °C (a, b), 25.5 °C (c, d) and 80 °C (e, f). These digital photos were taken with an immersion time of 1 h.

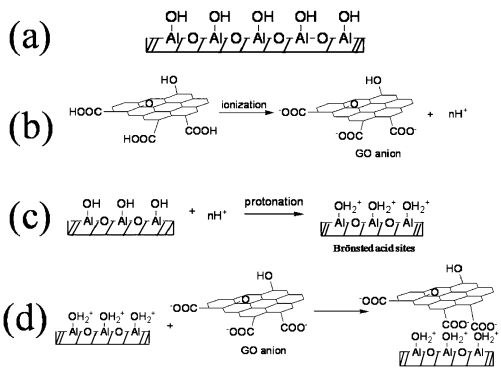

Fig. 3 Schematic of a tentative formation process of a GO hydrogel. (a) A fresh porous AAO surface; (b) ionization of GO; (c) protonation of hydroxylated AAO surface and (d) enrichment of GO nanosheets on AAO surface.

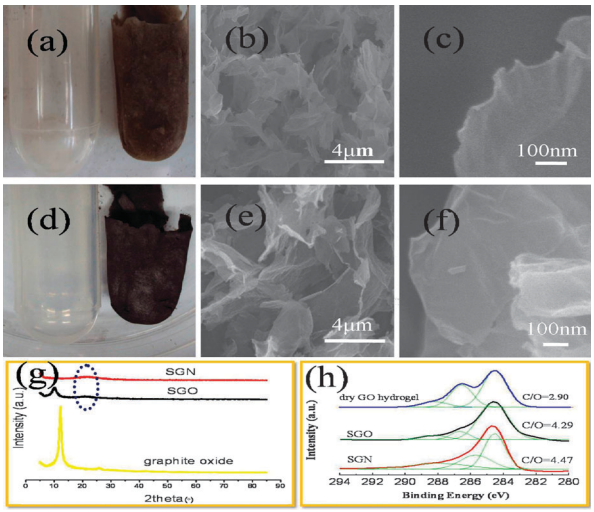

Fig. 4 Sponge-like macroform starting from a GO hydrogel formed on AAO surface. A digital photo (a) and SEM images (b, c) of a SGO; A digital photo (d) and SEM images (e, f) of a SGN; (g) XRD patterns of graphite oxide, SGO and SGN; (h) XPS C 1s profile of dry GO hydrogel, SGO and SGN.

sponge-like macroform (denoted as SGO) as shown in Fig. 4a. The obtained SGO is typical of a 3D network of overlapped GO nanosheets as revealed by SEM observations (Fig. 4b, c) and shows high methylene blue adsorption ability (320 mg g^{-1}) due to a large pore volume left by the removed water. XRD patterns (Fig. 4g) indicate an apparent difference between graphite oxide and SGO. Graphite oxide possesses a strong and sharp peak around 12.5°, typical for a layered structure of GO nanosheets. Comparatively, for a SGO, this peak becomes much weaker and shifts to a lower value (11°, an indication of larger interlayer spacing), which is well consistent with the random organization of GO nanosheets in a 3D network. A weak peak around 22° unexpectedly appears, indicative of a partial reduction of SGO in the lyophilization process, which is further confirmed by the XPS results (Fig. 4h) in which a larger C/O ratio is revealed compared with a dry GO hydrogel (ESI†). Two factors may contribute to the reduction process. The vacuum environment under lyophilization may promote the decomposition of some oxygen-containing groups on GO sheets while the loosened microstructure may give an escape path for the decomposed gaseous components. Investigations are ongoing to further clarify the interesting phenomenon (lyophilization-induced reduction). SGO was further reduced by a low-temperature annealing under vacuum[4a] and the resulting sample was denoted as SGN. The annealing process did not change the morphology of the sponge-like structure and Fig. 4d–f show typical optical and SEM images of SGN. For the reduced samples, only a broadened and weak peak around 22° is visible, which is attributed to partially overlapped graphene nanosheets. As shown in Fig. 4h, a peak around 286.5 eV is visible for a dry GO hydrogel in the XPS C 1s profile, which is related to abundant oxygen-containing groups. A decrease of the intensity of such a peak and an increase of C/O atomic ratios indicate a gradual reduction process from GO to SGN. SGN shows some potential as electrochemical energy storage media and preliminary results are presented in ESI (Fig. S5, ESI†).

In summary, a GO hydrogel is formed *via* an enrichment of GO nanosheets at a solid/liquid interface, and can be regarded as an ideal precursor for a sponge-like aerogel (SGO macroform) by lyophilization, which duplicates the macrotexture and microstructure of the parent hydrogel. The formation of such a GO hydrogel is mediated by a solid/liquid interfacial interaction between hydroxyl groups of AAO and carboxyl groups attached on GO sheets. The finally obtained SGN macroform by a reduction process with a low-temperature annealing shows a good electrochemical energy storage performance. Ongoing investigation is focused on the formation mechanism of the hydrogel and the potential application of the hydrogel and the sponge-like aerogel.

This work is financially supported by the National Natural Science Foundation of China (No. 50972101 and 51072131), Specialized Research Fund for the Doctoral Program of Higher Education (No. 20090032110014), the Project-sponsored by SRF for ROCS, SEM and Program of Introducing Talents of Discipline to Universities (No. B06006), China.

Notes and references

1 (*a*) A. K. Geim and K. S. Novoselov, *Nat. Mater.*, 2007, **6**, 183; (*b*) Y. Hernandez, V. Nicolosi, M. Lotya, F. M. Blighe, Z. Y. Sun, S. De, I. T. McGovern, B. Holland, M. Byrne, Y. K. Gun'ko, J. J. Boland, P. Niraj, G. Duesberg, S. Krishnamurthy, R. Goodhue, J. Hutchison, V. Scardaci, A. C. Ferrari and J. N. Coleman, *Nat. Nanotechnol.*, 2008, **3**, 563; (*c*) D. Li, M. B. Muller, S. Gilje, R. B. Kaner and G. G. Wallace, *Nat. Nanotechnol.*, 2008, **3**, 101.
2 C. Lee, X. D. Wei, J. W. Kysar and J. Hone, *Science*, 2008, **321**, 385.
3 Y. Wang, Y. Y. Shao, D. W. Matson, J. H. Li and Y. H. Lin, *ACS Nano*, 2010, **4**, 1790.
4 (*a*) W. Lv, D. M. Tang, Y. B. He, C. H. You, Z. Q. Shi, X. C. Chen, C. M. Chen, P. X. Hou, C. Liu and Q. H. Yang, *ACS Nano*, 2009, **3**, 3730–3736; (*b*) M. D. Stoller, S. J. Park, Y. W. Zhu, J. H. An and R. S. Ruoff, *Nano Lett.*, 2008, **8**, 3498.
5 N. L. Yang, J. Zhai, D. Wang, Y. S. Chen and L. Jiang, *ACS Nano*, 2010, **4**, 887.
6 F. N. Xia, D. B. Farmer, Y. M. Lin and P. Avouris, *Nano Lett.*, 2010, **10**, 715.
7 (*a*) K. P. Loh, Q. L. Bao, G. Eda and M. Chhowalla, *Nat. Chem.*, 2010, **2**, 1015; (*b*) Y. W. Zhu, S. Murali, W. W. Cai, X. S. Li, J. W. Suk, J. R. Potts and R. S. Ruoff, *Adv. Mater.*, 2010, **22**, 3906.
8 M. Quintana, K. Spyrou, M. Grzelczak, W. R. Browne, P. Rudolf and M. Prato, *ACS Nano*, 2010, **4**, 3527.
9 (*a*) C. M. Chen, Q. H. Yang, Y. G. Yang, W. Lv, Y. F. Wen, P. X. Hou, M. Z. Wang and H. M. Cheng, *Adv. Mater.*, 2009, **21**, 3541; (*b*) Z. J. Fan, J. Yan, L. J. Zhi, Q. Zhang, T. Wei, J. Feng, M. L. Zhang, W. Z. Qian and F. Wei, *Adv. Mater.*, 2010, **22**, 3723; (*c*) F. Kim, L. J. Cote and J. X. Huang, *Adv. Mater.*, 2010, **22**, 1954; (*d*) J. Kim, L. J. Cote, F. Kim, W. Yuan, K. R. Shull and J. X. Huang, *J. Am. Chem. Soc.*, 2010, **132**, 8180.
10 (*a*) M. K. Bayazit, L. S. Clarke, K. S. Coleman and N. Clarke, *J. Am. Chem. Soc.*, 2010, **132**, 15814; (*b*) Y. X. Xu, K. X. Sheng, C. Li and G. Q. Shi, *ACS Nano*, 2010, **4**, 4324.
11 (*a*) S. P. Adiga, P. Zapol and L. A. Curtiss, *J. Phys. Chem. C*, 2007, **111**, 7422; (*b*) K. C. Popat, G. Mor, C. A. Grimes and T. A. Desai, *Langmuir*, 2004, **20**, 8035; (*c*) Y. N. Pushkar, A. Sinitsky, O. O. Parenago, A. N. Kharlanov and E. V. Lunina, *Appl. Surf. Sci.*, 2000, **167**, 69.
12 (*a*) H. Bai, C. Li, X. L. Wang and G. Q. Shi, *Chem. Commun.*, 2010, **46**, 2376; (*b*) J. J. Liang, Y. Huang, L. Zhang, Y. Wang, Y. F. Ma, T. Y. Guo and Y. S. Chen, *Adv. Funct. Mater.*, 2009, **19**, 2297.
13 G. Eda and M. Chhowalla, *Adv. Mater.*, 2010, **22**, 2392.